On this basis, it is difficult to justify a barrier to rotation for the methyl groups in *tert*-butyl.

Consequences

The higher heats of formation or bond dissociation energies proposed here have important implications with respect to our understanding, at a fundamental level, of hydrocarbon cracking to olefins. With the available data base and thermokinetic considerations we have the basis for the complete quantitative description of the breakdown process in terms of elementary single-step reactions. In a sense this represents the "ultimate" chemical explanation of the phenomena. Indeed, the present results suggests that the data base for such understanding has existed for many years.

With these present results there can no longer be any doubt regarding the virtual absence of a barrier to ring closure for the cyclization of small hydrocarbon diradicals. Summarizing briefly, the enthalpy for ring opening during the decomposition of small ring compounds can be written as[49]

$$\Delta H(\text{ring opening}) = 2\Delta H(\text{alkane} \rightarrow \text{alkyl} + \text{H}) - \Delta H(\text{H}_2 \rightarrow 2\text{H}) + \Delta H(\text{hydrogenation, cyclane})$$

where the alkane is $HC_nH_{2n}H$ and the cyclane is C_nH_{2n}. Data for a number of representative compounds can be found in Table V. Also included are results on the cis-trans isomerization of olefins. Following Bergman,[49] we are treating these substances as a two-membered ring. There is very satisfactory agreement between the activation energy for ring opening and calculated results. Barriers to ring closing are reduced drastically. This is in striking contrast to the situation when the older bond energies are used. Bergman[49] and Berson[50] have discussed in detail the unreasonableness of the assumption of the barrier. A necessary consequence of the present results is a large reduction in the barrier to 1-2 hydrogen migration for the trimethylene radical during decomposition. The rates are thus much faster. Since these are fundamentally disproportionation reactions, this is to be expected. In the case of the tetramethylene diradical, the rate of β-bond scission is also increased since there is now no barrier to decomposition. This is in line with the tendency of the product olefins to retain some degree of the original conformation. With the older bond energies it is necessary to postulate a high barrier to internal rotation in order to rationalize the results. This is contrary to the expectation of minimal barriers to rotation of such systems.

(49) R. Bergman In "Free Radicals", Vol. 1, J. K. Kochi, Ed.; Wiley, New York, 1973, p 191.
(50) J. Berson In "Annual Reviews of Physical Chemistry", Annual Reviews, Inc. Palo Alto, CA, 1977, p 111.

Conclusions

The generaly conviction that measurements of the rate constants for alkyl radical decomposition suffer from gross errors is not correct. The misconception arises from an underestimation of the appropriate bond dissociation energies or heats of formation of the radicals in question. The higher values proposed here are supported by all available rate data from hydrocarbon decomposition and radical buffer studies. Results from iodination studies used as the basis for recently recommended values for radical heats of formation[8] lead to the implication that a great portion of the existing kinetic data on hydrocarbon systems which can be brought to bear on this question is in gross (orders of magnitude) error. This is difficult to believe inasmuch as results (from completely different experiments) are replicable. We have not been able to identify the source of error in the iodination experiments. Particularly disturbing is that the discrepancies are all in one direction. Nevertheless, our results suggest that one should be very cautious in the use of bond dissociation energies from iodination studies for quantitative purposes. Certainly, the present results would justify placing a 15 kJ uncertainty limit on many such values.

Acknowledgment. This work was supported by the Department of Energy, Division of Chemical Sciences, Office of Basic Energy Science under Interagency Agreement DE-A-101-76PR06010. I am grateful to D. M. Golden, D. F. McMillen, S. Lias, and S. E. Stein for careful reading of the manuscript and many useful comments.

Chirality of the Electron Density Distribution in Methyl Groups with Local C_3 Symmetry

Alberto Gutiérrez, James E. Jackson, and Kurt Mislow*

Contribution from the Department of Chemistry, Princeton University, Princeton, New Jersey 08544. *Received October 9, 1984*

Abstract: The chirotopicity of methyl groups with local C_3 symmetry cannot be expressed in the static point-nuclear distribution. We now report ab initio (6-31G) calculations for twisted ethane (D_3) and 1,1,1-trifluoroethane (C_3) that reveal a chiral distortion of the electron distribution throughout the CH_3 group. The effect is small but may be implicated in chirality phenomena and chiral discriminations.

Molecular models may be cut into chiral or achiral segments whose symmetries are subgroups of the molecular point group.[1,2] In the general model of the molecule, the local chirality (chirotopicity) of such a segment is observable in the nuclear and electron distribution functions.[2] Where the nuclei form a chiral array, the electron distribution is expected to follow suit. However, under the assumption of the point-nuclear model, there are cases in which the δ distribution of nuclear positions does not allow a distinction between chirotopic and achirotopic subarrays.[3] In such cases the distinction can come from a consideration of the electron distribution. In this paper we show the manifestation of such an effect

(1) Anet, F. A. L.; Miura, S. S.; Siegel, J.; Mislow, K. *J. Am. Chem. Soc.* **1983**, *105*, 1419. This segmentation is an abstract and purely geometric operation and not a chemical fragmentation.
(2) Mislow, K.; Siegel, J. *J. Am. Chem. Soc.* **1984**, *106*, 3319.
(3) Let m be the *minimum* number of points that are required to define a chiral array of points in E^3 ($m \geq 4$). Then m is equal to the order of the symmetry group for arrays with D_n, T, O, or I symmetry and equal to twice the order of the group for C_n ($n > 1$) symmetry ($m = 4$ for C_1). For example, $m = 12$ for C_6, D_6, or T symmetry.

0002-7863/85/1507-2880$01.50/0

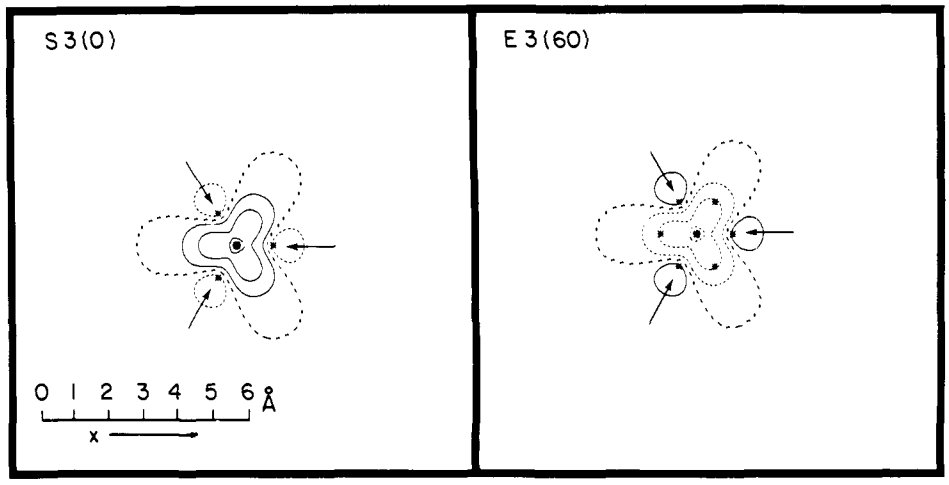

Figure 1. S3(0) and E3(60) CDD plots for ethane. The view is from above the C-1 methyl group looking from C-1 toward C-2 along the C–C bond axis. Asterisks indicate the atom positions of the specified geometry (0°-ethane for S3(0) and 60°-ethane for E3(60)) projected onto the plane. Arrows mark the projected C-1 methyl hydrogen positions.[13] A scale of angstroms and the direction of the x axis are shown in the lower left corner. Solid contour lines indicate excess electron density in the scrutinized conformation, dotted lines indicate an excess in the reference structure, and the dashed line is the zero contour. Contour levels (in electron/bohr^3) are as follows: 0.0, ±0.000316, ±0.001, ±0.00316, ±0.01, ±0.0316, ±0.1, ±0.316, ±1.0.

in the case of the methyl group with local C_3 symmetry.

Chirotopic Methyl Groups. Chirotopic CH_3 groups may possess either local C_1 or local C_3 symmetry.[4] Those with local C_1 symmetry (C_1-CH_3) are ubiquitous in chemistry and biochemistry and are encountered in structures ranging from natural products, such as the steroids and terpenes, to simple achiral molecules, such as 2-propanol. In the static model of these molecules, the local chirality of C_1-CH_3 groups is distinguished by the asymmetric distribution of the four atoms. In contrast to such groups, the array of four point-nuclei in methyl groups with local C_3 symmetry (C_3-CH_3) is indistinguishable from an *achiral* array of point-nuclei.[3] Under static conditions, the local chirality of such a methyl group can therefore be best expressed by the electron distribution function.[5]

Effects due to the chirotopicity of C_3-CH_3 groups should in principle be experimentally observable, e.g., as chiroptical phenomena in the vibrational region of the electromagnetic spectrum.[6] However, to our knowledge no such observations have been reported to date. Alternatively, it might be possible to detect the chirality of the electron density distribution in C_3-CH_3 as obtained by high-quality MO calculations. The present work was undertaken in order to investigate this possibility. We chose to search for a chirality effect in D_3-ethane, the simplest structure containing C_3-CH_3 groups, and in C_3-1,1,1-trifluoroethane.

Methods

The GAUSSIAN 82 series of programs[7,8] was used in this work. Calculations on ethane and 1,1,1-trifluoroethane were performed within the RHF approximation with the 6-31G basis set of Hehre, Ditchfield, and Pople.[9,10] Bond lengths and bond angles were fixed at the literature values reported for the optimized structures (staggered) of ethane (6-31G*)[12a] and 1,1,1-trifluoroethane (3-21$^+$G).[12b] For each molecule, wave functions were then obtained for the seven geometries generated by decrementing the HCCH or HCCF torsion angle from staggered (60°) to eclipsed (0°) in steps of 10°, while keeping bond lengths and bond angles frozen.

A set of total charge density grids, T, was computed for each structure in a series of five parallel planes, perpendicular to the C–C axis and defined as follows: (1) the plane containing the three hydrogen atoms attached to C-1;[13] (2) the plane halfway between C-1 and plane 1; (3) the plane containing C-1; (4) the plane halfway between the C–C midpoint and C-1; and (5) the plane bisecting the C–C bond. Each plane was oriented so that the projections of the carbon atoms were at the origin, with one of the C-1 methyl hydrogen atom projections falling along the plane's x axis. Thus the C-1 methyl group projection was positioned identically in each plane for various orientations of the C-2 methyl or CF_3 group. Two sets of charge density difference (CDD) plots were then computed by subtraction of the set of five density grids of a reference geometry from the set for the geometry of interest; the reference geometries (staggered or eclipsed) were chosen so that the methyl groups had local C_{3v} symmetry. Set S was generated by using the staggered conformation as the reference (subtracted) geometry. Set E arose in the same manner, except that the eclipsed conformation replaced the staggered as the reference geometry. In each subtraction, coincidence of corresponding nuclei in the two C-1 methyl groups was ensured by superposition of the projected atom positions. Thus the CDD plots in sets S and E depict the displacement of charge density in the region of the C-1 methyl group upon rotation of the C-2 methyl or CF_3 group from its reference position (staggered or eclipsed) to the selected torsion angle. A given set (T, E, or S), plane (1–5), and torsion angle (0–60°) combination is specified as in the following examples. S1(40) indicates set S (which uses the staggered conformation as its subtracted reference), plane 1 (the plane of the three H atoms), and the 40° conformation (i.e., torsion angle HCCH or HCCF = 40°) as the geometry under scrutiny. Similarly, E5(10) specifies a plot of the charge density difference between the 10° conformation and the eclipsed structure at the C–C bond midpoint plane, and T3(30) refers to the total charge density plot for the 30° conformation in the plane through C-1.

Examples of CDD plots obtained by this method are shown in Figure 1. The figure on the left, S3(0), shows the plot obtained by superposition and subtraction in plane 3 of the staggered ethane C-1 methyl group density from the C-1 methyl group density in the eclipsed structure; the figure on the right, E3(60), obtained by subtracting eclipsed from staggered densities, is simply the negative of the plot for S3(0). Both plots

(4) The highest symmetry attainable by pyramidal CH_3 is C_{3v}, and chiral subgroups are therefore limited to C_1 and C_3.

(5) We note, however, that in molecules such as **1**, C_3-CH_3 chirotopicity is maintained even under conditions of rapid internal rotation. See: Franzen, G. R.; Binsch, G. *J. Am. Chem. Soc.* **1973**, *95*, 175.

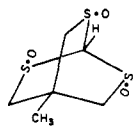

1

(6) The chirality of the nuclear and electronic distributions in C_1-CH_3 groups is experimentally detectable by Raman circular intensity differential spectroscopy. See: Barron, L. D.; Vrbancich, J. *Top. Current Chem.* **1984**, *123*, 151 and references therein.

(7) GAUSSIAN 82: Release A. Binkley, J. S.; Frisch, M.; Krishnan, R.; Defrees, D. J.; Schlegel, H. B.; Whiteside, R.; Fluder, E.; Seeger, R.; Pople, J. A., Copyright 1982, Carnegie-Mellon University.

(8) The authors are grateful to Professor L. C. Allen for making the GAUSSIAN 82 program[7] available to users at Princeton.

(9) Hehre, W. J.; Ditchfield, R.; Pople, J. A. *J. Chem. Phys.* **1972**, *56*, 2257.

(10) Preliminary calculations using the polarized 6-31G* basis set[11] showed negligible differences from the 6-31G results.

(11) Harihan, P. C.; Pople, J. A. *Theor. Chim. Acta* **1973**, *28*, 213.

(12) (a) Wiberg, K. B.; Wendoloski, J. J. *J. Am. Chem. Soc.* **1982**, *104*, 5679. (b) Schleyer, P. v. R.; Kos, A. J. *Tetrahedron* **1983**, *39*, 1141.

(13) In this paper, C-1 refers to the carbon atom in the methyl group under scrutiny. According to this convention, C-1 in 1,1,1-trifluoroethane corresponds to C-2 in the IUPAC name of the compound.

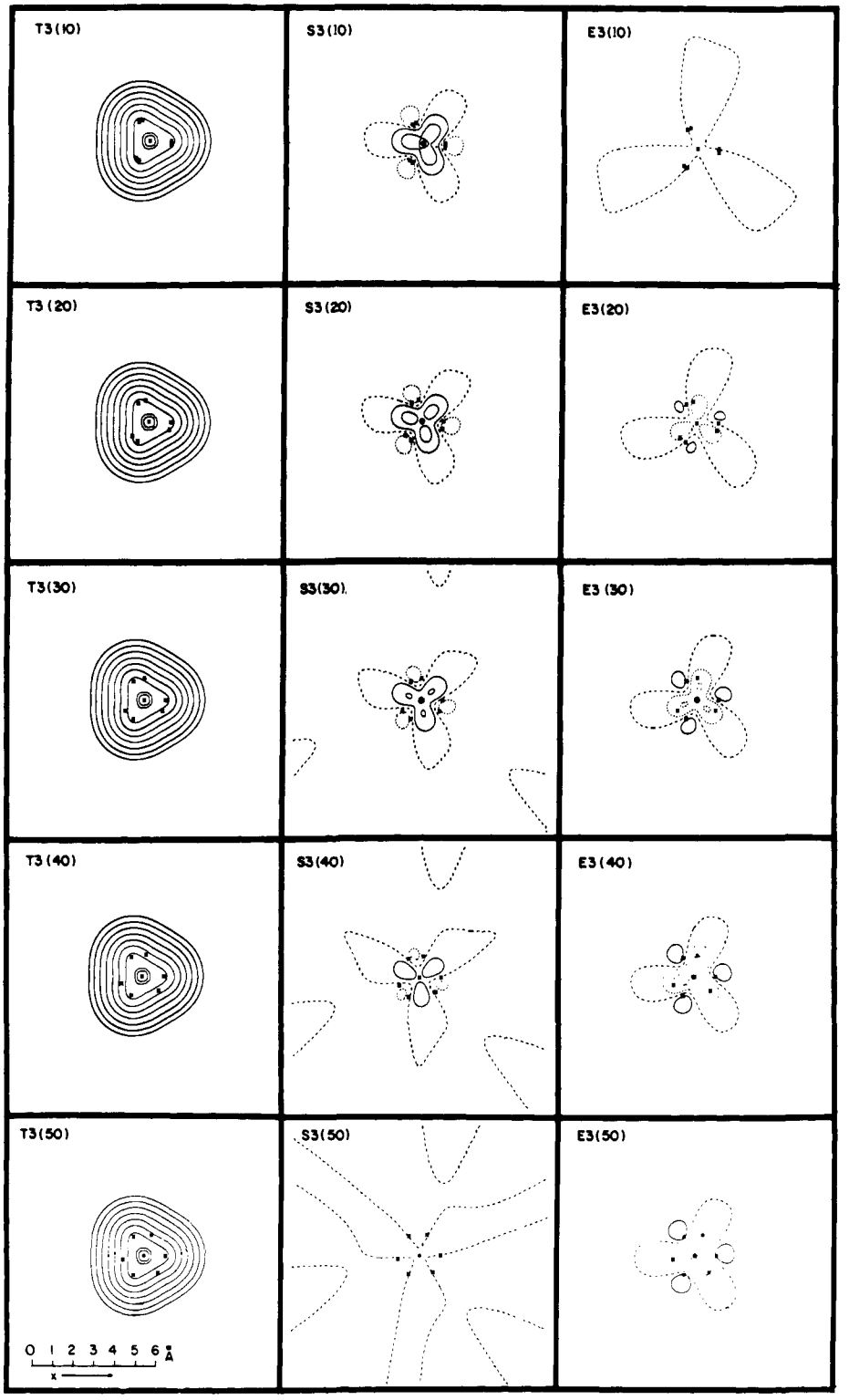

Figure 2. Variation of electron density distribution in the plane through C-1 in ethane as a function of the HCCH torsion angle. See the Methods section and Figure 1 for an explanation of the notation and plots.

trace out achiral patterns with exact planar D_3 symmetry.[14]

Results and Discussion

***D_3*-Ethane.** In principle, it should be possible to detect chirality in the total charge density grid (T) of the CH_3 group in D_3-ethane. Accordingly, we began our study by computing T plots for all five planes in each of five chiral conformations, corresponding to torsion angles of +10, +20, +30, +40, and +50°. Figure 2 (left column) shows the results for the variation of T3 as a function of torsion angle. To the eye, all these contour plots appear to be indistinguishable and achiral (planar D_3 symmetry). Figure 3 (left column) shows the results for the variation of T(40) as a function of the position of the plane along the C–C axis. A slight variation in the appearance of the contour plots is now discernible, but once again they all appear to possess planar D_3 symmetry.[15]

(14) In the euclidean plane, achiral D_3 symmetry is exemplified by an equilateral triangle and chiral C_3 symmetry by a triskelion.

(15) Note that the pattern of each of the T plots for planes 1–4 (T1(40)–T4(40)) appears achiral (planar D_3 symmetry), with a mirror line along the x axis. In the plot for T5(40), which has exact planar D_3 symmetry, the corresponding mirror line is rotated 20° from the x axis; thus, the five T plots in combination constitute a helical array that reflects the chirality of the C_3-CH_3 moiety.

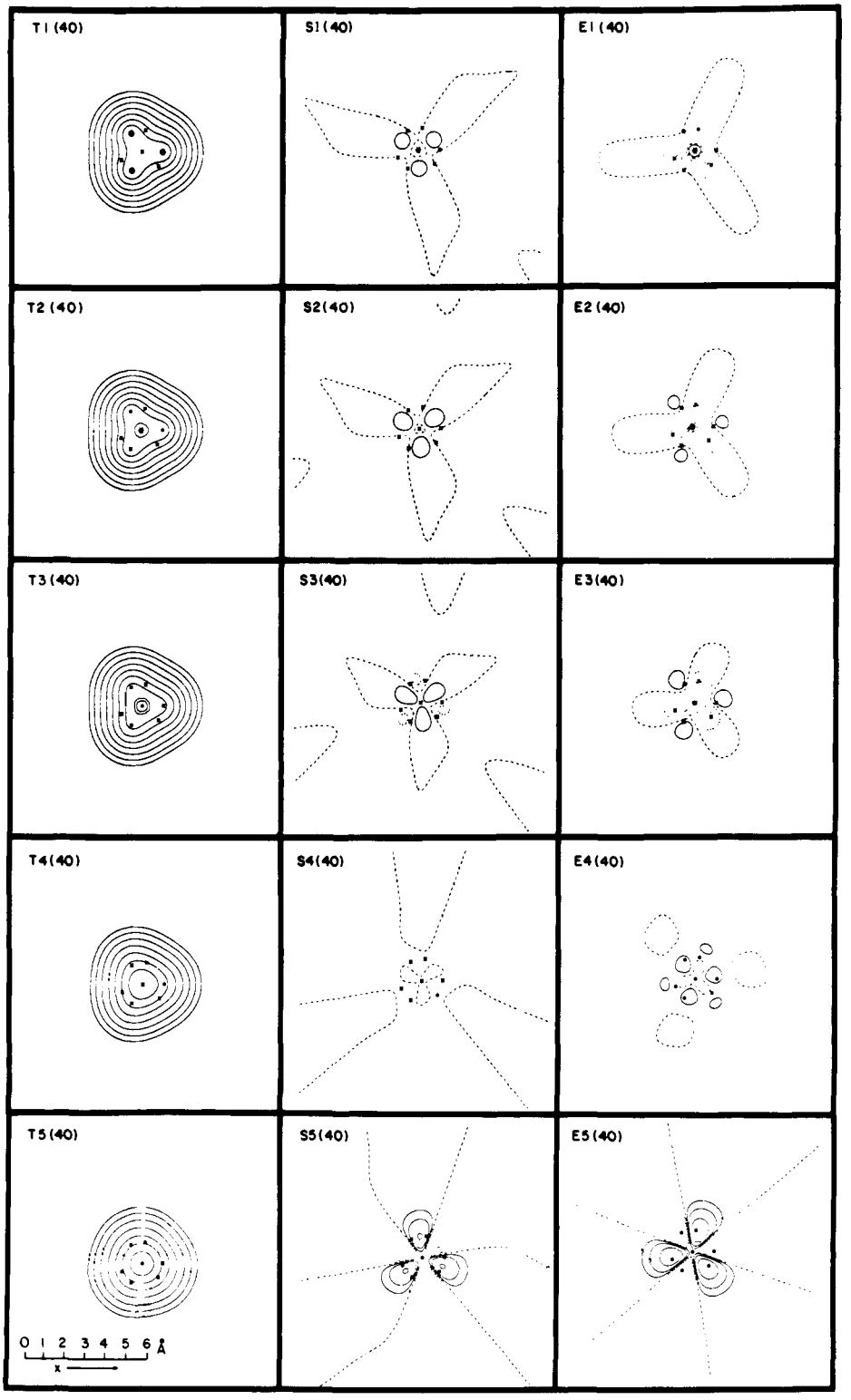

Figure 3. Variation of electron density distribution in 40°-ethane as a function of the position of the plane along the C–C bond axis. See the Methods section and Figure 1 for an explanation of the notation and plots.

These nine examples are typical of the results that were obtained for all 25 combinations: in no case was there any visual evidence for chirality in the T plots. Evidently, the chiral perturbation of one methyl group by the other is quite weak and is completely overshadowed by the magnitude of the total electron density.

To visualize the chiral nature of the total charge densities, we resorted to the stratagem of subtracting the electron density in the achirotopic CH_3 group (local C_{3v} symmetry) of D_{3d}- or D_{3h}-ethane from the electron density in the chirotopic CH_3 group (local C_3 symmetry) of D_3-ethane. The procedure is described in the Methods section. Typical results are displayed in the center and right columns of Figures 2 and 3.

Figure 2 shows CDD plots in plane 3 as a function of the torsion angle. We note that the absolute magnitude of the CDD's decreases from S3(10) to S3(50), becoming zero by definition at S3(60), and that there is an analogous decrease from E3(50) to E3(10), with the CDD vanishing at E3(0). Not surprisingly, S3(10) and E3(50) closely resemble the achiral plots (Figure 1) for S3(0) and E3(60), respectively, but the patterns of the eight remaining CDD plots, S3(20)–S3(50) and E3(10)–E3(40), unmistakably convey the triskelion character of planar C_3 symmetry.

The chiral distortion effects thus uncovered are not restricted

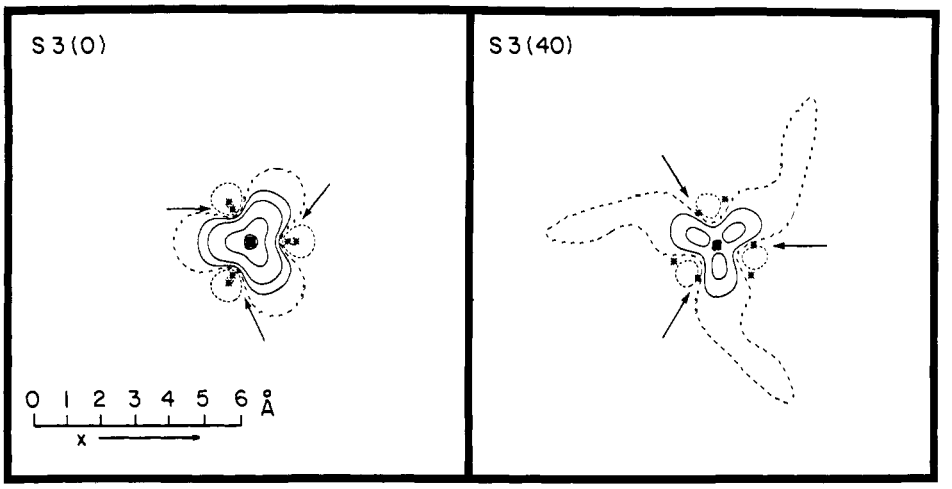

Figure 4. S3(0) and S3(40) CDD plots for 1,1,1-trifluoroethane. For further explanations, see the Methods section and Figure 1.

to plane 3, as can be seen by inspection of the CDD plots in Figure 3: the patterns of the S(40) CDD plots for all five planes (center column) are strikingly chiral, and similar effects, though less pronounced, are exhibited by the patterns of the E(40) CDD plots (right column).[16]

The 18 examples of CDD's in Figures 2 and 3 are typical of the results obtained for all 50 combinations. In short, *the chirotopicity of the C_3-CH_3 groups in D_3-ethane clearly manifests itself in the chirality of the CDD plots.*[17,18]

C_3-1,1,1-Trifluoroethane. An MO study of this molecule was undertaken on the assumption that substitution of the strongly polar and relatively electron-rich CF_3 group for the weakly perturbing C-2 methyl group in D_3-ethane might result in a substantial enhancement of the chiral perturbation in the C-1 methyl group. Accordingly, T and CDD plots (reference geometries: staggered and eclipsed C_{3v}-1,1,1-trifluoroethane) were computed for the C-1 methyl group.[13] All five planes in each of five chiral (*P*) conformations were examined, as described for ethane. As before, to the eye all 25 T contour plots appear to be achiral (planar D_3 symmetry). However, the CDD plots are now more strikingly chiral,[19] as illustrated by the planar C_3 symmetry of the S3(40) plot in Figure 4. Reference to the S3(40) plot for ethane (Figure 3) reveals the differential effect of the electron density in the CF_3 group on the CDD of the CH_3 moiety.

Comparison of the S3(0) plot for 1,1,1-trifluoroethane (Figure 4) with that for ethane (Figure 1) shows that the achiral electronic reorganization accompanying the twist from 0° to 60° is greater (by a factor of ca. 3) in trifluoroethane than in ethane. By separating these radial and longitudinal contributions to the CDD's from the purely torsional components which give the plots their triskelion character, one may estimate and compare the magnitude of the chiral effect in ethane and trifluoroethane.[20] In the 30° and 40° structures, the purely torsional components of the electronic distortions in trifluoroethane are 1.5–1.8 times as large as those calculated for ethane. Thus substitution of fluorine for hydrogen appears to affect the torsional electronic distortion considerably less than it does the longitudinal and radial components.

Quantitative Considerations and Conclusion. To obtain a rough estimate of the chemical relevance of the electronic distortions examined in this work, we may compare the torsional and longitudinal displacements discussed for ethane and trifluoroethane with the deformation density calculated at 6-31G for the C–C bond in staggered ethane. The torsional distortion maximum in 30°-ethane is ca. 1.5×10^{-4} e$^-$/bohr^3, while in 30°-trifluoroethane it is ca. 2.3×10^{-4} e$^-$/bohr^3.[21] The corresponding longitudinal distortion calculated for rotation from 60° to 0° is ca. 1.0×10^{-3} e$^-$/bohr^3 for ethane and ca. 3.2×10^{-3} e$^-$/bohr^3 for trifluoroethane. Finally, the deformation density maximum for the C–C bond in staggered ethane is ca. 4.0×10^{-2} e$^-$/bohr^3. Thus, the torsional electron density reorganization accompanying a 30° twist in ethane is on the order of 1/400 to 1/200 the magnitude of that due to C–C σ bond formation in ethane and roughly 1/10 of the magnitude of that due to the geometry change from staggered to eclipsed. Because the deformation density maximum and the longitudinal distortion maximum for ethane are in essentially the same ratio (30:1) as the corresponding C–C bond homolysis energy and ethane rotational barrier, it is tempting to suggest that the chiral effects correspond to an energy change of roughly 0.3 kcal/mol.

The results of the present work, though predestined on grounds of symmetry, clearly demonstrate that the chirotopicity of molecular segments is expressed in the chiral distortion of the electron density distribution, even under circumstances where the δ nuclear distribution in the segment is achiral. This type of perturbation underlies all chirality phenomena or chiral discriminations that arise from effects of the molecular environment on chirotopic

(16) For sets S(40) and E(40), planes 1–4 show relatively small changes in electron density in the locale of the C-1 methyl group. However, as in the T set,[15] plane 5 begins to show the much larger electronic distortion resulting from the subtraction of the non-superposed C-2 methyl groups.

(17) The sense of chirality of the plots in Figures 2 and 3 depends on the orientation of the viewer relative to the projection plane (see Figure 1) as well as on the absolute configuration (*P*) of the D_3-ethane.

(18) The triskelion character of the electron density distribution in C_3-methyl groups may be expressed by a bent-bond variant of the familiar Newman projection

(19) In operational usage, "chiral" and "achiral" become fuzzy concepts that may be properly rank-ordered. See: Mislow, K.; Bickart, P. *Isr. J. Chem.* **1976/1977**, *15*, 1.

(20) This separation was accomplished by averaging right- and left-handed T3(30) and T3(40) charge densities for each molecule, to give a set of achiral densities which incorporated the longitudinal and radial distortions for the selected torsion angles. The achiral average so obtained was subtracted from the corresponding T charge density to give a contour map of a purely torsional distortion. Algebraically these plots arise from the following type of subtraction

$$\text{Torsional density} = \text{T3(30)} - \tfrac{1}{2}[\text{T3(30)} + \text{T3(-30)}]$$

which may be simplifed to

$$\tfrac{1}{2}[\text{T3(30)} - \text{T3(-30)}]$$

(21) The 30° conformations and plane 3 were selected as the cases which would show the greatest torsional electronic distortion.

segments, such as optically active transitions in chromophoric segments of chiral molecules.[22] Our results accord with the view[2] that a segment has no identity outside of its identity as a part of the molecule and that the symmetry of such a segment is inseparable from that of its environment.

Acknowledgment. We thank the National Science Foundation (CHE-8009670) for support of this work and J. Siegel for helpful discussions. One of us (J.E.J.) thanks Princeton University for the award of a Charlotte Elizabeth Procter Fellowship.

Registry No. Ethane, 74-84-0; 1,1,1-trifluoroethane, 420-46-2.

(22) Mason, S. F. "Molecular Optical Activity and the Chiral Discriminations"; Cambridge University Press: Cambridge, 1982.

Molybdenum(VI)-Dioxo, Molybdenum(V)-Oxo, and Molybdenum(IV)-Oxo Complexes with 2,3:8,9-Dibenzo-1,4,7,10-tetrathiadecane. Models for the Molybdenum Binding Site of the Molybdenum Cofactor

Bharat B. Kaul,[1a] John H. Enemark,[1b] Shannath L. Merbs,[1b] and J. T. Spence*[1a]

Contribution from the Department of Chemistry and Biochemistry, Utah State University, Logan, Utah 84322, and the Department of Chemistry, University of Arizona, Tucson, Arizona 85721.
Received October 22, 1984

Abstract: As possible models for the coordination of molybdenum by an unsaturated thiolate-thioether ligand in the molybdenum-pterin cofactor of molybdenum enzymes, MoO_2(dttd), MoOCl(dttd), and MoO(PPh_2Et)(dttd) (dttdH_2 = 2,3:8,9-dibenzo-1,4,7,10-tetrathiadecane) have been synthesized. The structure of MoO_2(dttd) has been determined by X-ray crystallography. The compound crystallizes in space group $P2_1/c$, with a = 14.34 (2) Å, b = 8.168 (6) Å, c = 14.507 (8) Å, β = 103.42 (8)°, and Z = 4. MoO_2(dttd) is six-coordinate with substantial distortion from octahedral geometry. The two thiolate S atoms are trans to one another (Mo-S_{av} = 2.402 (7) Å) and cis to the terminal oxo groups. The thioether S atoms are approximately trans to the terminal oxo groups and exhibit much longer Mo-S distances (2.687 (6) Å). MoO_2(dttd) undergoes a one-electron reversible reduction on the cyclic voltammogram time scale, but is reduced irreversibly in the presence of Et_4NCl in a two-electron step to [MoOCl(dttd)]$^-$ on the coulometric time scale; [MoOCl(dttd)]$^-$ in turn is reversibly oxidized to the EPR active monomer MoOCl(dttd). MoOCl(dttd) undergoes a reversible one-electron reduction to [MoOCl(dttd)]$^-$, but cannot be oxidized to MoO_2(dttd) in the voltage range used. MoO(PPh_2Et)(dttd) appears to lose the PPh_2Et group in DMF/Et_4NCl solution, exhibiting electrochemical behavior identical with that of [MoOCl(dttd)]$^-$. Reaction of MoO_2(dttd) with 1 equiv of PPh_2Et in DMF in the presence of Et_4NCl gives [MoOCl(dttd)]$^-$, while subsequent addition of Me_2SO to the solution regenerates MoO_2(dttd). The dimer, Mo_2O_3(dttd)$_2$, has also been obtained. It is reversibly reduced in a 1.00 electron/Mo process to [MoOCl(dttd)]$^-$ and reversibly oxidized in a 0.50 electron/Mo process to a mixture of equal amounts of MoO_2(dttd) and MoOCl(dttd) in DMF in the presence of Et_4NCl. The EPR parameters of MoOCl(dttd) and the electrochemical parameters of the various complexes are reported.

Molybdenum is an essential component of a number of enzymes that catalyze two-electron redox processes.[2,3] These enzymes have a common cofactor,[4,5] a small molybdenum-containing molecule that can be released by acid treatment of one enzyme and added to a second apoenzyme to give an active species. Recent work has identified a novel reduced pterin with a sulfur side chain from the cofactor[6] and has led to a proposed structure of the cofactor with molybdenum bound to the side chain:

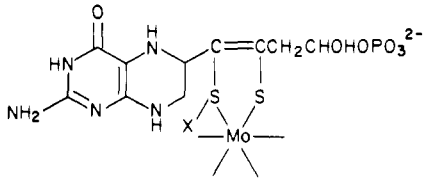

X = Me if present

Recent electronic and CD spectroscopic studies of the molybdenum domain of sulfite oxidase suggest the presence of an unusual Mo-sulfur ligand, giving some support to this structure.[7] If X = Me, the molybdenum is coordinated by an α,β-unsaturated β-mercapto thioether, a ligand type not previously reported for Mo(VI)-dioxo or Mo(V)- and (IV)-oxo complexes. Furthermore, EXAFS results have indicated two or three thiolate groups and possibly a thioether are present as ligands on molybdenum in sulfite oxidase.[8] Only two Mo(VI)-dioxo complexes and no Mo(V)- or Mo(IV)-oxo complexes with thioether coordination have been previously reported; the determination of bond lengths, electrochemical properties, and EPR parameters for such complexes is therefore of considerable interest with respect to thioether coordination in Mo enzymes.

We report here the synthesis and properties of oxomolybdenum(VI), -(V), and -(IV) complexes of 2,3:8,9-dibenzo-1,4,7,10-tetrathiadecane (dttdH_2), an S_4 tetradentate ligand

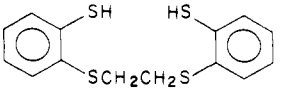

dttdH_2

with aromatic thiolate-thioether groups.[9] This is the first use

(1) (a) Utah State University. (b) University of Arizona.
(2) Bray, R. C. *Adv. Enzymol. Relat. Areas Mol. Biol.* **1980**, *51*, 107.
(3) Hewitt, E. J.; Notton, B. A. In "Molybdenum and Molybdenum Containing Enzymes"; Coughlan, M., Ed.; Peramon Press: New York, 1980; p 273. Ljungdahl, L. G. *Ibid.* p 463.
(4) Wahl, R. C.; Rajaopalan, K. V. *J. Biol. Chem.* **1982**, *257*, 1354.
(5) Johnson, J. L. In "Molybdenum and Molybdenum Containing Enzymes"; Coughlan, M., Ed.; Pergamon Press: New York, 1980; p 347.
(6) Johnson, J. L.; Rajagopalan, K. V. *Proc. Natl. Acad. Sci. U.S.A.* **1982**, *79*, 6856.
(7) Garner, C. D.; Buchanan, I.; Collison, D.; Mabbs, F. E.; Porter, T. G.; Wynn, C. H. In "Proceedings of the 4th International Conference on the Chemistry and Uses of Molybdenum"; Barry, H. F., Mitchell, P. C. H., Eds.; Climax Molybdenum: Ann Arbor, 1982; p 163.
(8) Cramer, S. P.; Wahl, R.; Rajagopalan, K. V. *J. Am. Chem. Soc.* **1981**, *103*, 7721.

0002-7863/85/1507-2885$01.50/0